V

Publication V

The formation and characterisation of ultra-thin films containing Ag nanoparticles†

Kirsi Yliniemi,[a] Marjatta Vahvaselkä,[b] Yves Van Ingelgem,[c] Kitty Baert,[c] Benjamin P. Wilson,[a] Herman Terryn[c] and Kyösti Kontturi*[a]

A simple three step method for creating ultra-thin films, which contain Ag nanoparticles, on both glass and stainless steel surfaces, is presented. First, during the immersion into N-(2-aminoethyl)-3-aminopropyl-trimethoxysilane (DIAMO) a monolayer of DIAMO is attached on the sample surface after which immersion in silver nitrate is performed and a complex between the two amino groups of DIAMO and silver ions forms, leading to large clusters on the surface. During the annealing step these silver containing clusters are converted into silver nanoparticles which are homogeneously distributed and bound to the surface. The formation of the film was characterised using UV/Vis, FE-SEM and FE-AES. Additionally, SERS activity of the surface and the effect of the attachment of the nanoparticles on their antibacterial nature were also investigated.

Introduction

There is a wide variety of possible applications for Ag nanoparticles, including for example the incorporation of silver nanoparticles on the surfaces for antibacterial purposes,[1–3] SERS (surface-enhanced Raman scattering) surfaces[4–7] as well as use in optical switches[8] and dry (photo)thermographic processes.[9–11]

However, at the same time with the development of new applications of metallic nanoparticles there is increased concern of the possible health risks due to nanoparticle exposure.[12,13] Therefore, there exists a clear need for surface modifications in which the nanoparticles are attached to the surface and the diffusion of nanoparticles to the surrounding environment is therefore inhibited. On the other hand this raises the question as to whether these attached nanoparticles still possess their superior capabilities.

The main purpose of this study was to develop a simple method for surface modifications with attached silver nanoparticles by using a modified layer-by-layer (LbL) process. The resulting surfaces have been characterised by a number of complimentary techniques and the SERS activity as well as the influence of the attached nanoparticles on their antibacterial action have been studied.

LbL type methods, which were developed by the pioneers Netzer and Savig[14] and Mallouk and co-workers,[15,16] provide an interesting approach for developing new functional surfaces. It has been exploited in the formation of both SERS substrates[4,17–19] and antibacterial surfaces[20,21] where metal nanoparticles have been incorporated into these films. This has been achieved by using pre-prepared nanoparticle sols[4,5,22–24] or reducing metal ions inside LbL films either with NaBH$_4$ solution[1,25] or heating in H$_2$ atmosphere.[26] However, to the best of the authors' knowledge, antibacterial surfaces comprise layers in which nanoparticles are weakly associated giving rise to the strong possibility of nanoparticle diffusion into the surrounding environment. The in-situ approach presented here not only simplifies the process by the use of di-amino functionalised trimethoxysilane that provides both the attachment to the surface and the reduction of the nanoparticles during annealing, but more importantly produces films in which nanoparticles are attached on the surface.

As mentioned previously LbL techniques have also been used to produce SERS active surfaces. In general, two widely accepted explanations have been given for the mechanism of SERS: chemical and electromagnetic enhancements.[27] Enhancement is also believed to be due to so-called hot particles[28] and Kneipp et al.[29] have estimated that only 0.01% of the molecules in the sample are involved in the enhancement. It has also been found that when the silver nanoparticles are immobilised on a polyvinylpyridine modified glass substrate the enhancement is affected by the surface attachment when compared to that seen for a colloidal suspension.[18]

The antibacterial effects of silver nanoparticles and silver ions have also been subjects of much debate in recent years and there are contradictory results as to the antibacterial properties of silver ions and silver nanoparticles.[3,30–33] A study by Simonetti et al.[32] suggests that only silver ions have a strong antibacterial effect but silver in the form of a neutral salt is not such a potent antibacterial agent. However, several substrates incorporating silver nanoparticles have shown antibacterial properties. For example, Shi et al.[3] have reported that the

[a]Laboratory of Physical Chemistry and Electrochemistry, Helsinki University of Technology, P.O. Box 6100, FI-02015 TKK, Finland. E-mail: kyosti.kontturi@tkk.fi; Fax: +358 9 451 2580; Tel: +358 9 451 2570
[b]Laboratory of Biochemistry and Microbiology, Helsinki University of Technology, P.O. Box 6100, FI-02015 TKK, Finland
[c]Dept. Metallurgy, Electrochemistry and Materials Science, Vrije Universiteit Brussel V.U.B., Pleinlaan 2, 1050 Brussels, Belgium
† Electronic supplementary information (ESI) available: 1) A typical AFM image and height profile of the annealed sample surface; 2) maps of N and Si peak intensities measured by FE AES of the pure DIAMO coated sample. See DOI: 10.1039/b713313h

antibacterial effect of N-hexyl-N-(4-vinylbenzyl)-4,4'-bipyridinium dinitrate (HVVN) was enhanced in the presence of Ag nanoparticles.[3] In addition, Dai and Bruening[1] have been able to create Ag nanoparticle containing electrocatalytically active and antibacterial films of polyethyleneimine–metal complex/poly(acrylic acid). These results suggest that both the films with Ag$^+$ ions and those containing nanoparticles work as antibacterial materials. Furthermore, according to them, nanoparticle loaded films are preferred to reduce the harmful diffusion of Ag$^+$ ions into the body.[1]

Panáček et al.[31] have studied the antibacterial activity of silver colloids with different size distributions and according to them the smallest i.e. 25 nm sized nanoparticles were the most effective. The antibacterial mechanism is unknown but they believe that silver nanoparticles might attach on the surface of the cell membrane, disturbing its power function (permeability and respiration). The penetration of nanoparticles inside the bacteria is also suggested, however the release of silver ions is not excluded as a possibility.[31] Rubner and co-workers,[20,21] on the other hand, have studied the antibacterial effect of multilayers of nanoparticles and the results indicate that nanoparticles are required for the slower release of an antibacterial substance, which is, however, the silver ion rather than the nanoparticle itself. According to them, the rate determining step is the oxidation of zero-valent Ag and not the diffusion of silver ions in the film.[20]

In addition to the attachment of nanoparticles onto the surface, there are also other benefits of the method adopted in this work. When compared to more traditional sol–gel methods, the films are extremely thin (only a few monolayers), are easily synthesized and a non-complex chemistry of the film is achieved. Above all, the original surface appearance can be maintained, which is of prime importance for applications like medical devices that need to be both hygienically and aesthetically clean.

Experimental

Chemicals and materials

The chemicals were used as received and were the following: AgNO$_3$ (99.8% p.a. Merck), Methanol (MeOH, 99.9% p.a. Merck), N-(2-aminoethyl)-3-aminopropyl-trimethoxysilane (DIAMO, 97% Merck), NH$_3$ (25%, Merck), H$_2$O$_2$ (30%, Fluka), tetrahydrofuran (THF, HPCL Grade Rathburn), 2-propanol (99.8% p.a. Fluka), ethanol (EtOH, A Altia), HCl (1 M, Merck). Water used in the hydrolyzing in DIAMO was MQ water.

The ultra-thin films were prepared either on Menzel-Gläser microscope glass slides (Menzel GmbH) or stainless steel (AISI 304, Outokumpu Stainless) surfaces. The glass samples were alkaline cleaned prior to use in a solution of NH$_3$ + H$_2$O$_2$. Stainless steel samples were both solvent cleaned (twice for 15 min in ultrasonic bath in the each solvent: 1) THF, 2) 2-propanol, 3) EtOH) and alkaline cleaned before use.

Synthesis

The preparation of the samples was carried out in three steps. Step 1: clean samples were exposed to DIAMO for 24 h and then rinsed carefully with methanol and dried by a stream of N$_2$. Step 2: samples were then dipped for 24 h into the solution of 0.50 g AgNO$_3$ + 20 ml MeOH, which had been stirred for an hour prior to use. The beaker was wrapped in aluminium foil as silver nitrate is light sensitive. After 24 h the samples were rinsed again carefully with MeOH and dried with N$_2$. Step 3: finally, the nanoparticles were produced on the surface by annealing the samples in air at 120 °C.

Characterisation

The effect of annealing for different periods of time was investigated with UV/Vis spectroscopy and spectra were measured in either transmission mode (Perkin Elmer Lambda 2) for glass substrates or reflectance mode (Perkin Elmer Lambda 950) for stainless steel substrates. The spectra on stainless steel were obtained using an integrating sphere, which leads to the observation of absorbance as a negative peak since both the reflected and scattered beams were collected by the sphere.

Further surface characterisation of the film was performed with field emission scanning electron microscopy (FE SEM) and Auger electron spectroscopy (FE AES) using a JEOL JSM 7000-F and a JEOL JAMP 9500-F spectroscope respectively. These were used to produce secondary electron images and elemental surface maps of the elements present on the steel surface. In both types of analysis the electron source was a field emission gun generating a primary beam energy of 10 keV. For Auger analysis a current of 0.35 nA was applied and for the depth profile of the final film the sputter rate of 3 nm min^{-1} was used (calibrated on SiO$_2$). Two different kinds of samples were studied: 1) DIAMO + Ag$^+$ clusters on the surface (after Step 2, prior to annealing) and 2) DIAMO + Ag nanoparticles on the surface (after Step 3, annealed for 2 h at 120 °C). In addition, Si and N maps were measured on the surface of the pure DIAMO coated sample (after Step 1, annealed at 120 °C, 2 h) to check the coating uniformity. Also atomic force microscopy (AFM) was used to determine the size of the nanoparticles on the surface; only the sample after Step 3 (annealed at 120 °C for 2 h) was studied.

Ag$^+$ ion dissolution tests were carried out using four glass samples (size 1 × 3 cm^2) after Step 2 (prior to annealing) and four glass samples after Step 3 (after annealing at 120 °C for 2 h). The samples were placed into two separate test tubes both containing MQ water to find the difference of Ag$^+$ ion dissolution from these two types of samples. After 24 h the samples were removed and the solutions were analysed by inductively coupled plasma atomic emission spectroscopy (ICP-AES, Varian Liberty). The wavelength for Ag analysis was 338.289 nm.

SERS activity tests

To test the SERS activity of the produced surfaces, a Raman spectrum of the films was obtained in 10^{-4} M solution of phenylmercaptotetrazole (PMT). This type of solution is suited very well to investigating the SERS activity of silver containing surfaces.[34] Additionally, the SERS spectra of samples with thicker DIAMO + Ag nanoparticle films as well as of a known SERS probe were measured. The SERS probe (developed

in-house at the Vrije Universiteit Brussel) consisted of silver particles in a gelatine matrix on a glass substrate ensuring good SERS enhancement.[35] The thicker films were prepared exactly in the same way as ultra-thin films except pre-hydrolysed DIAMO was used instead of pure DIAMO in Step 1. The pre-hydrolysis of DIAMO was performed in a manner similar to that employed by Delattre *et al.*:[36] the HCl solution (pH = 2) was added into a DIAMO–MeOH solution (molar ratio of MeOH : DIAMO = 2 : 1) resulting in a molar ratio of H_2O : DIAMO = 3:1 and the solution was stirred for 24 h. Using this pre-hydrolysed DIAMO it was possible to prepare films containing more DIAMO and silver. The SER spectra were obtained on a DILOR XY spectrometer equipped with an Olympus microscope (magnification of $50 \times$, focal length of 8 mm), a single monochromator, a notch filter and a liquid nitrogen cooled charge-coupled device detector with resolution of ~ 2 cm^{-1}. Excitation was provided by the 514 nm radiation of a Coherent Innova 70C argon–krypton mixed gas laser. The output power was 25 mW for the stainless steel samples, and 12 mW for the SERS probe. The background signal was subtracted and the spectra were normalized as a function of the most intense peak.

Antibacterial activity tests

The antibacterial experiments were performed with *Escherichia coli* VTT E-94564 and *Micrococcus luteus* TKK 10611. The bacteria were cultivated in Nutrient broth No. 2 (LabM) at 37 °C for 18 h (*E. coli*) or at 30 °C for 24 h (*M. luteus*). Two different kinds of samples were studied: 1) DIAMO + Ag^{+} clusters on the surface (after Step 2, prior to annealing) and 2) DIAMO + Ag nanoparticles on the surface (after Step 3, annealed for 2 h at 120 °C) prepared on glass slides (size 1×3 cm^2). The glass slides were placed in sterile test tubes and 4.5 ml of Nutrient broth inoculated with *E. coli* or *M. luteus* to the level of 500 colony forming units (CFU) per ml was added. The tubes were incubated at 37 °C (*E. coli*) or 30 °C (*M. luteus*) with 150 rpm agitation for 24 h. For comparison, inoculated Nutrient broth without glass slides was also incubated. The tests were performed in triplicate. Samples for viable counts were taken at 1, 5 and 24 h (*E. coli*) or at 5 h (*M. luteus*). Viable counts were determined by plating on Nutrient agar (LabM) and the plates were incubated at 37 °C for 24 h (*E. coli*) or at 30 °C for 48 h (*M. luteus*). The results are reported as the means of log (CFU ml^{-1}) and standard deviations (SD). The student's *t*-test was used to evaluate statistically significant differences ($p < 0.05$).

Results and discussion

Characterisation of the ultra-thin films

Silver nanoparticles have a surface plasmon resonance peak at a wavelength around 400 nm. The placement of the peak is dependent on several factors, such as size and shape of the particles and also the surrounding matrix. Fig. 1a shows the UV/Vis transmission spectra of the glass substrate as a function of annealing time in air at 120 °C. The small shoulder is observed around 400 nm already without any annealing but a clear and narrow peak starts to form after 30 min at 120 °C
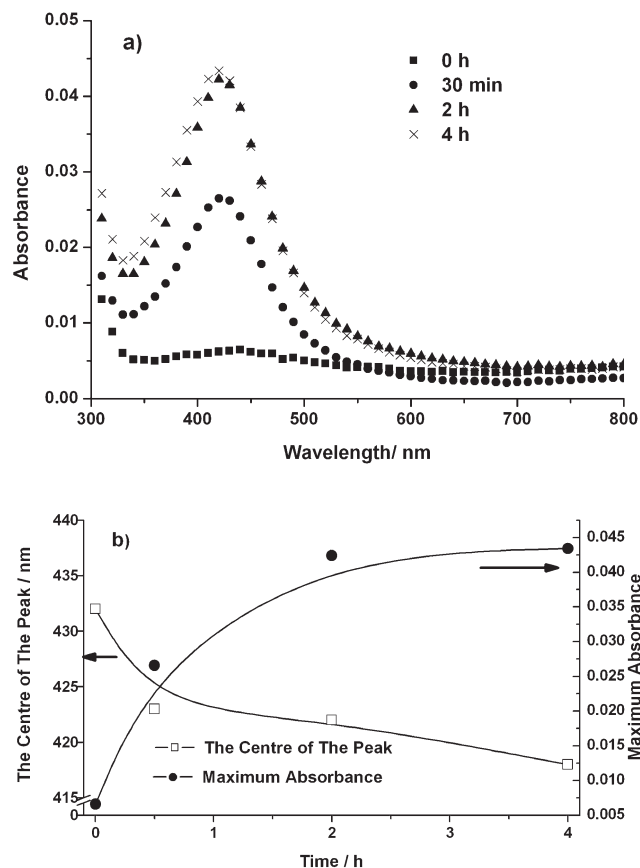
Fig. 1 a) The absorbance spectra of the formation of Ag nanoparticles on glass surface as a function of annealing time at 120 °C. b) The change of the centre of the plasma resonance peak of Ag nanoparticles on the glass surface (left axis) and the maximum absorbance of the plasma resonance peak (right axis) as a function of the annealing time at 120 °C. The solid line is present for illustrative purposes.

indicating the formation of Ag nanoparticles on the surface. The absorbance increases and the centre of the peak is blue-shifted from approximately 435 nm to 420 nm during two hours of annealing, after which the peak shape and position do not change anymore. This blueshift is clearly illustrated in Fig. 1b which shows the changes in the centre of the peak and the maximum absorbance as a function of annealing time.

Fig. 2a shows the UV/Vis spectra of a stainless steel substrate as a function of the annealing time. The negative peak can be correlated to the surface plasmon resonance peak of Ag nanoparticles around 400 nm and it starts to form after 30 min of annealing. A similar trend to that for the glass substrate is observed as the shape and position of the peak do not change remarkably after the first two hours. Also, during the formation of nanoparticles on the stainless steel surface, the centre of the peak is shifted from approximately 435 nm to 420 nm similar to glass surfaces within 4 h of annealing. Fig. 2b shows the changes in the centre of the peak and the minimum reflectance as a function of the annealing time.

Both the reflectance and absorbance values are very low due to the extremely small amount of Ag present on the surface. The films were prepared with careful methanol rinsing, after both the DIAMO and methanol + AgNO$_3$ immersion, and
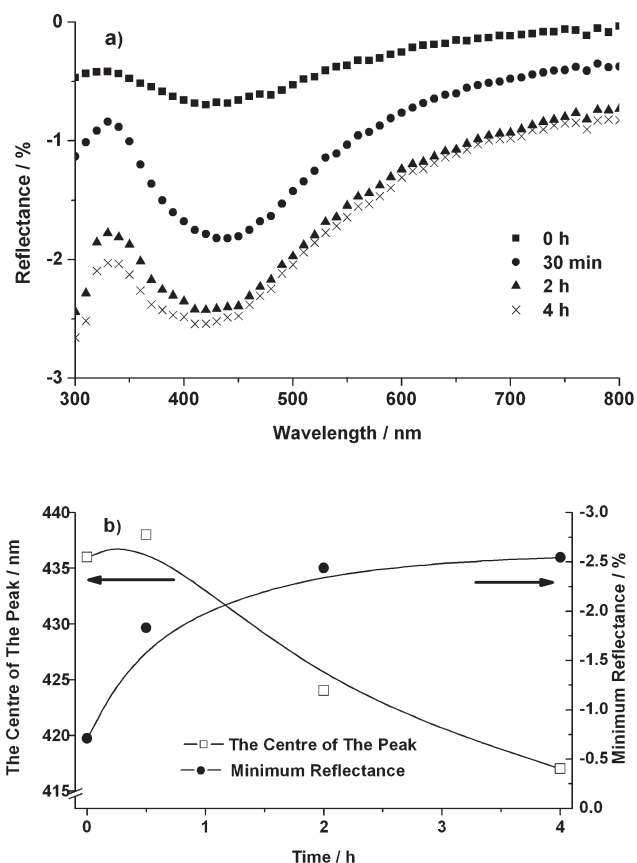
Fig. 2 a) The UV/Vis spectra of the formation of Ag nanoparticles on stainless steel surface as a function of annealing time at 120 °C. b) The change of the centre of the plasma resonance peak of Ag nanoparticles on the stainless steel surface (left axis) and the minimum reflectance of the plasma resonance peak (right axis) as a function of the annealing time at 120 °C. The solid line is present for illustrative purposes.

therefore only the attached monolayer of DIAMO and later silver nanoparticles are believed to stay on the surface. Furthermore a comparison of Fig. 1 and 2 demonstrates that the nanoparticles form in a similar manner both on the insulating glass and the conductive stainless steel surfaces indicating that the formation has to take place by reaction with DIAMO and the nature of the substrate does not play a crucial role.

It is known that silver forms a $[Ag(NH_3)_2]^+$ complex when dissolved in an ammonia solution.[37] For example, nanoparticle sols have been prepared from a dissolved silver complex by reducing with different saccharides similar to the so-called Tollens process or silver mirror test.[31,38] Therefore the formation of a silver complex with the two amino groups of DIAMO is expected to take place when a DIAMO coated sample is immersed into methanol + $AgNO_3$ solution for 24 h. The reduction of the silver complex is thought to take place simultaneously with the polymerisation of DIAMO during the annealing step as non-attaching methoxy/silanol groups of DIAMO are cleaved in a way similar to the basic silanisation process.[39] However, in contrast to the normal silanisation process, the procedure presented here contains no pre-hydrolysing of DIAMO. Here only a small portion of pure DIAMO has spontaneously hydrolysed and can attach to the

surface resulting in an ultra-thin film. Furthermore, the Ag nanoparticles are believed to be attached to DIAMO as it is known to act as an effective binder between gold nanoparticles and silica particle surfaces.[40] DIAMO has also been used as a stabiliser for gold nanoparticles[41] as well as for silver nanoparticles in sol–gel matrices.[42,43] Results from Ag^+ ion analysis with ICP-AES show that the dissolution from samples which contain mainly Ag^+ ions (after Step 2, prior to annealing) is significantly higher than from the samples which contain Ag nanoparticles (after Step 3, annealed at 120 °C for 2 h)—1.5 mg l^{-1} vs. 0.4 mg l^{-1}, respectively—and therefore indicates that the nanoparticles are attached on the surface via DIAMO molecules. The exact nature of the nanoparticle attachment is still open to interpretation and not the subject of this particular paper.

The reaction path introduced above resembles the one used in dry (photo)thermographic processes in which silver ions are reduced on the surface of a photographic plate during annealing in the presence of binders, stabilisers and reducers.[9–11] Formation of Ag_xO_y particles cannot be totally excluded as the preparation is carried out in air and residual nitrates possibly present in the clusters could decompose during heating into AgO and NO_x.

To achieve confirmation of the reaction path introduced above, further studies were made with FE SEM and FE AES. Fig. 3a and b show the SEM images of the stainless steel surface after Step 2 (prior to annealing) and after Step 3 (annealed at 120 °C for 2 h), respectively. The non-annealed sample contains larger clusters when compared to the annealed sample on which there are more but smaller clusters observed. This result correlates with the UV/Vis data, which show the formation of nanoparticles as a function of annealing time. The size of nanoparticles was estimated from atomic force microscope images (see electronic supplementary information (ESI),† Fig. S1): the average height of the particles is 6–9 nm and average diameter is approximately 35 nm.

Whether the clusters in Fig. 3a and b contain silver or not cannot be distinguished from SEM images alone and therefore the behaviour during annealing was further investigated with FE AES. Fig. 4a and b introduce Ag peak intensity maps of the stainless steel samples both after Step 2 (prior to annealing) and after Step 3 (annealed for 2 h at 120 °C), respectively. The FE AES maps confirmed the findings from SEM images as large silver aggregates can be observed on the surface (Fig. 4a) of the non-annealed sample and these clusters are expected to contain mainly Ag^+ ions and only relatively few nanoparticles (related to the small shoulder in UV/Vis spectra). In addition, some nitrates may be involved in the clusters (the silver amino complex is positively charged) to balance the electroneutrality condition. When the non-annealed sample (Fig. 4a) is compared to the annealed sample (Fig. 4b) it can be seen that during the annealing the clusters have re-formed to silver nanoparticles. The nanoparticles are more homogeneously distributed on the surface than the clusters and the estimated surface coverage of silver was up to 5%.

One of the main advantages of the silver nanoparticle films prepared in this way is the formation of ultra-thin, almost invisible films. The depth profiles determined by FE AES show the average thickness of the film to be 4.7 nm. This is
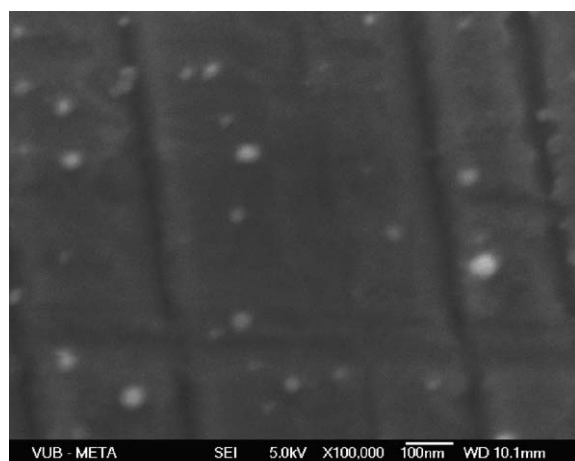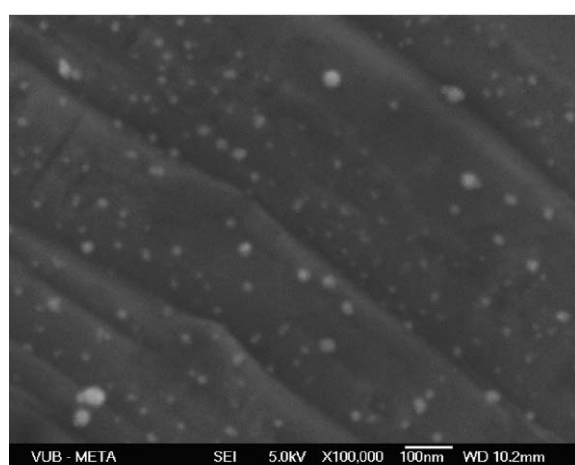
Fig. 3 SEM images of the stainless steel surfaces with a) DIAMO + Ag⁺ clusters, prior to annealing, b) DIAMO + Ag nanoparticles, annealed at 120 °C for 2 h.

confirmed by measuring Fe peak intensity maps of the non-annealed and annealed samples, which are presented in Fig. 5a and b, respectively. Fig. 5 shows that Fe can be detected uniformly for both annealed and non-annealed samples. As further proof of the film's ultra-thin nature, maps of both N and Si intensities on pure DIAMO coated sample (after Step 1 plus annealing for 2 h at 120 °C) were measured to confirm that DIAMO forms a uniform coating (see ESI† Fig. S2a and b, respectively). Therefore it can be concluded that Fe on the surface in Fig. 5a and b is more likely detected through the DIAMO monolayer than from the holes as would be the case with a non-uniform DIAMO coating.

Fig. 6 shows a schematic model which summarises how the film is formed during the preparation procedure. First, a monolayer of DIAMO is formed on the surface. Then, Ag–amino complexes are formed while immersed in AgNO$_3$ solution. The annealing at 120 °C in air creates Ag nanoparticles, which are attached to the surface by the DIAMO layer. Between every step the sample is rinsed carefully with methanol.

SERS activity

In addition to the surface characterisation, the SERS activity of the samples was studied. Fig. 7 shows the Raman spectra of (a) a known SERS probe prepared in-house at VUB, (b) a thicker film containing Ag nanoparticles, prepared by the same method as for the ultra-thin films but using *pre-hydrolysed* DIAMO, and (c) an ultra-thin film containing silver nano-particles (after Step 3, annealed for 2 h at 120 °C). The SERS active molecule used was phenylmercaptotetrazole (PMT) and the concentration of the solution was 1×10^{-4} M.

The SERS probe shows a typical SERS spectrum of PMT but as can be seen, no enhancement was observed when the spectrum was measured on the ultra-thin film. However, when measuring on the thicker film (prepared using pre-hydrolysed DIAMO) a clear SERS spectrum similar to the one measured
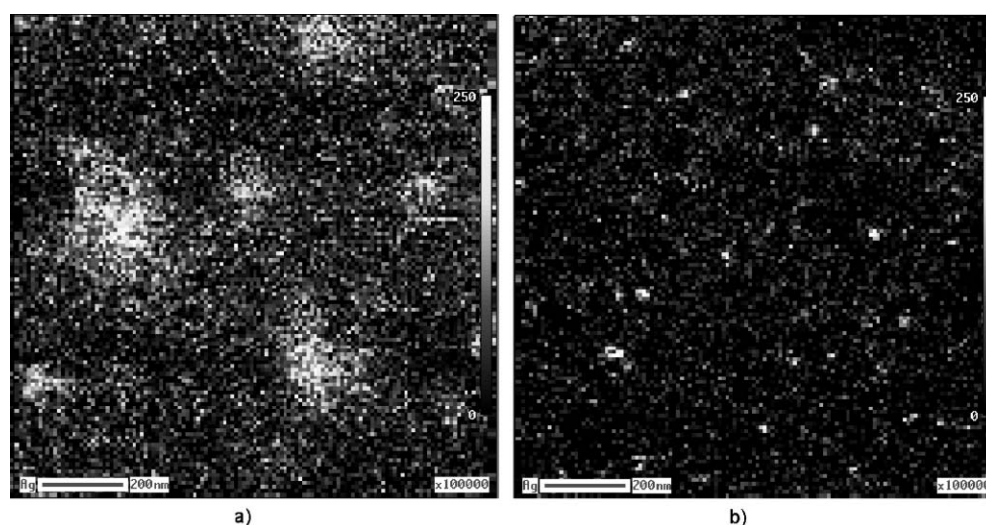
Fig. 4 Maps of Ag peak intensity of a sample containing a) DIAMO + Ag⁺ clusters, prior to annealing and b) DIAMO + Ag nanoparticles, annealed at 120 °C for 2 h.
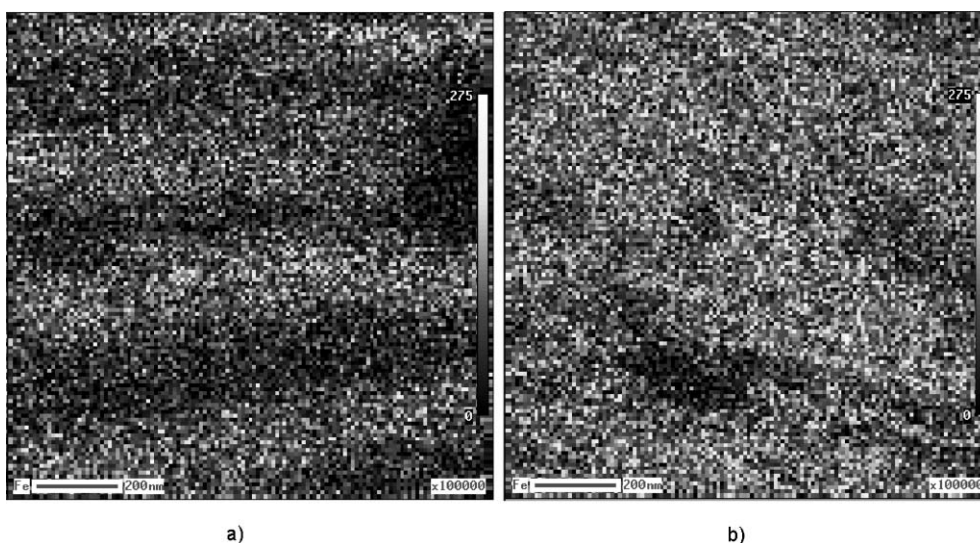
Fig. 5 Maps of Fe peak intensity of a sample containing a) DIAMO + Ag⁺ clusters, prior to annealing and b) DIAMO + Ag nanoparticles, annealed at 120 °C for 2 h.
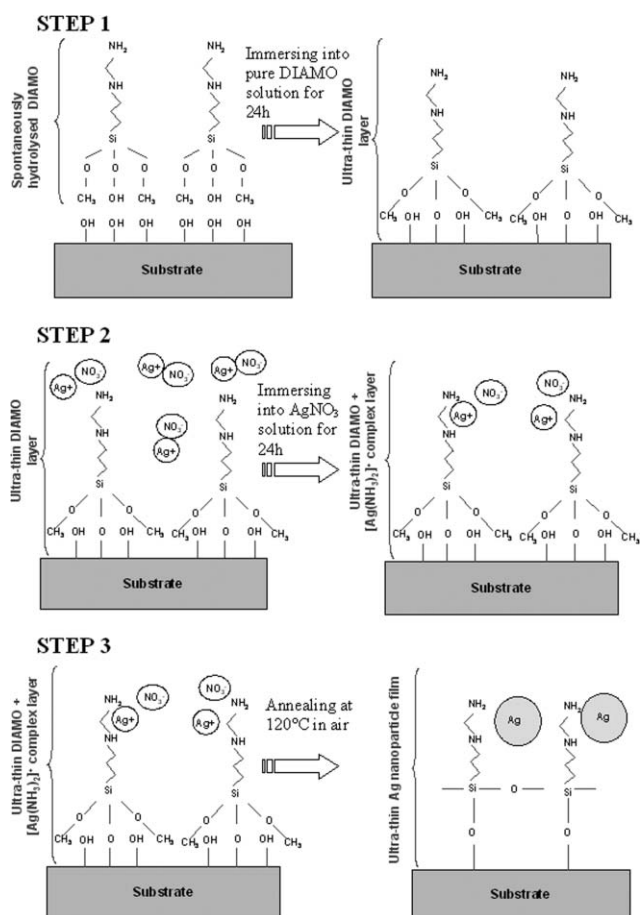
Fig. 6 Schematic diagram of the ultra-thin film formation on the substrate surface.

Fig. 7 Raman spectra of a) a known SERS probe, b) a thicker film prepared exactly the same as ultra-thin films but using pre-hydrolysed DIAMO and c) an ultra-thin film.

The main reason for the difference between the thicker films and ultra-thin films is believed to be due to greater amount of Ag nanoparticles on the surface as the thicker films are yellow in colour and can be seen easily even by the naked eye (unlike the ultra-thin films). As mentioned previously, usually only a small portion of the molecules are adsorbed on the hot spots,[28,29] so the enhancement is detectable only when a greater amount of Ag nanoparticles are present to create SERS active areas. This clearly demonstrates that a modification of the procedure with a pre-hydrolysing step is useful for the preparation of SERS active surfaces.

Antibacterial activity

The effect of Ag nanoparticles and Ag⁺ ions attached to glass slides on bacterial growth was studied by the viable count in nutrient broth inoculated with a low level of bacterial cells. These test conditions were chosen, as they allow the study of

with the SERS probe is seen. The SERS enhancement factors have been calculated[44] and for the probe it is approximately 8×10^7 and for the thicker film (prepared using pre-hydrolysed DIAMO) it is 1×10^7.

Table 1 Effects of silver ions or silver nanoparticles in ultra-thin films on growth of *Escherichia coli* in Nutrient broth: Sample 1) Ag^+ ions on glass (after Step 2, prior to annealing), Sample 2) Ag nanoparticles on glass (after Step 3, annealed for 2 h at 120 °C), Sample 3) control (no glass slide)[a]

Sample	0 h	1 h	5 h	24 h
1	2.33 ± 0.07	2.22 ± 0.20	4.68 ± 0.85[b]	9.23
2	2.33 ± 0.07	2.15 ± 0.29	5.52 ± 0.71	9.15
3	2.33 ± 0.07	2.50 ± 0.19	6.28 ± 0.13[b]	9.48

[a] Results are expressed as means ± SD of log (CFU ml^{-1}) values. [b] Statistically significant difference ($p < 0.05$).

both bacteriostatic and bacteriocidal, *i.e.* bacterial growth inhibiting and cell killing, modes of action. The commonly used methods[45] for testing antimicrobial activity, *e.g.* agar diffusion test and minimum inhibitory concentration (MIC) broth test, do not reveal the nature of inhibition of the antimicrobial agent without further testing of the viability of the inoculated cells.

The film containing Ag^+ ions on the glass slides (after Step 2, prior to annealing) inhibited the growth of the gram-negative *Escherichia coli* during the first hours of incubation since at 5 h the difference in viable counts as compared to the control was statistically significant ($p < 0.05$) (Table 1). Also the Ag nanoparticles on the glass slides (after Step 3, annealed for 2 h at 120 °C) seemed to cause a slight inhibition in growth, but without statistical significance. All the incubated cultures grew to high cell densities overnight indicating that the initial bacteriostatic action of Ag^+ ions was transient.

The glass slides containing either Ag^+ ions or Ag nanoparticles on the surface did not show bactericidal properties in the nutrient broth together with *E. coli* cells as incubation for 1 h did not cause a statistically significant reduction in viable counts.

The gram-positive *Micrococcus luteus* strain proved to be more resistant against both of the silver preparations when tested under similar conditions. After 5 h incubation, the log viable counts had increased from 2.76 ± 0.18 to 2.99 ± 0.13 in the presence of Ag^+ ions, to 3.16 ± 0.11 with the Ag nanoparticles, and to 3.12 ± 0.05 in the control. The differences between these increments are not statistically significant.

Results of the antibacterial tests reflect the nature of silver nanoparticles on the surface. Therefore, these findings suggest that the attached silver nanoparticles themselves do not posses antibacterial activity but, instead, sufficient release of ions is necessary. This is in contrast to findings from earlier studies which suggest that Ag nanoparticle containing films are antibacterial, although there is no discussion of the fact that the antibacterial behaviour is due to Ag^+ ions from dissolution of Ag nanoparticles rather than the nanoparticle itself[1,3] or of the unwelcome diffusion of Ag nanoparticles from the films into the surrounding environment before the dissolution step.[20] The results presented here address this, and it is also worth noting that antibacterial action of bound nanoparticles could still occur when bacterial cells in a non-growing state are adhered to the studied Ag nanoparticle surfaces.

Conclusions

A three step method for producing ultra-thin films containing Ag nanoparticles on stainless steel and glass surfaces has been outlined. A straightforward synthesis involving DIAMO layer adsorption, followed by immersion into $AgNO_3$ solution and subsequent annealing at 120 °C results in an ultra-thin film in which silver clusters transform to nanoparticles during the annealing step. These nanoparticles are homogeneously distributed and believed to be strongly attached to the surface. Samples possessing SERS activity can also be prepared by this method when pre-hydrolysed DIAMO to produce thicker films is used and the amount of silver content is increased on the surface. Finally, the current communication encourages further debate as to the actual origin of antibacteriality with Ag nanoparticles and their modes of action; whether the undesirable dissolution of Ag nanoparticles is needed or if the dissolution of Ag^+ ions occurs in sufficient amounts directly from the still attached nanoparticles to be effective. As highlighted by this paper, it demands the application of different antibacterial testing systems than those generally applied in which the dissolution of silver has an overriding influence on the final results. The findings presented here show that an antibacterial effect of films with bound silver nanoparticles is not observed in the studied testing system, but an additional step involving reduction and silver ion release is required.

References

1 J. Dai and M.L. Bruening, *Nano Lett.*, 2002, **2**, 497.
2 Q. Wang, H. Yu, L. Zhong, J. Liu, J. Sun and J. Shen, *Chem. Mater.*, 2006, **18**, 1988.
3 Z. Shi, K. G. Neoh and E. T. Kang, *Langmuir*, 2004, **20**, 6847.
4 R. F. Aroca, P. J. G. Goulet, D. S. dos Santos, R. A. Alvarez-Puebla and O. N. Oliveira, *Anal. Chem.*, 2005, **77**, 378.
5 M. D. Musick, C. D. Keating, L. A. Lyon, S. L. Botsko, D. J. Peña, W. D. Holliway, T. M. McEvoy, J. N. Richardson and M. J. Natan, *Chem. Mater.*, 2000, **12**, 2869.
6 J. K. Daniels and G. Chumanov, *J. Phys. Chem. B*, 2005, **109**, 17936.
7 K. Kim and J. K. Yoon, *J. Phys. Chem. B*, 2005, **109**, 20731.
8 P. Chakraborty, *J. Mater. Sci.*, 1998, **33**, 2235.
9 E. Tourwé, Towards a quantitative description of electrochemical reactions: a spectro-electrochemical study of the reduction of silver ions, Ph.D Thesis, Vrije Universitet Brussel, Brussels, 2005, pp. 3–13.
10 A. S. Diamond and D. S. Weiss, *Handbook of Imaging Materials*, 2nd edn, Marcel Dekker, New York 2002, pp. 473–529.

11 T. Maekawa, M. Yoshikane, H. Fujimura and I. Toya, *J. Imaging Sci. Technol.*, 2001, **45**, 365.
12 P. H. M. Hoet, I. Brüske-Hochfeld and O. V. Salata, *J. Nanobiotechnol.*, 2004, **2**, 1.
13 M. N. Moore, *Environ. Int.*, 2006, **32**, 967.
14 L. Netzer and J. Savig, *J. Am. Chem. Soc.*, 1983, **105**, 674.
15 H. Lee, L. J. Kepley, H.-G. Hong and T. E. Mallouk, *J. Am. Chem. Soc.*, 1988, **110**, 618.
16 H. C. Yang, K. Aoki, H.-G. Hong, D. D. Sackett, M. F. Arendt, S.-L. Yau, C. M. Bell and T. E. Mallouk, *J. Am. Chem. Soc.*, 1993, **115**, 11855.
17 N. P. W. Peczonka, P. J. G. Goulet and R. F. Aroca, *J. Am. Chem. Soc.*, 2006, **128**, 12626.
18 Q. Zhou, Q. Fan, Y. Zhuang, Y. Li, G. Zhao and J. Zheng, *J. Phys. Chem. B*, 2006, **110**, 12029.
19 D. Pristinksi, S. Tan, M. Erol, H. Du and S. Sukhishvili, *J. Raman Spectrosc.*, 2006, **37**, 762.
20 D. Lee, R. E. Cohen and M. F. Rubner, *Langmuir*, 2005, **21**, 9651.
21 Z. Li, D. Lee, X. Sheng, R. E. Cohen and M. F. Rubner, *Langmuir*, 2006, **22**, 9820.
22 C. Lu, S. Bai, D. Zhang, L. Huang, J. Ma, C. Luo and W. Cao, *Nanotechnology*, 2003, **14**, 680.
23 K. Esumi, S. Akiyama and T. Yoshimura, *Langmuir*, 2003, **19**, 7679.
24 L. Supriya and R. O. Claus, *J. Phys. Chem. B*, 2005, **109**, 3715.
25 D. Lee, R. E. Cohen and M. F. Rubner, *Chem. Mater.*, 2005, **17**, 1099.
26 S. Joly, R. Kane, L. Radizilowski, T. Wang, A. Wu, R. E. Cohen, E. L. Thomas and M. F. Rubner, *Langmuir*, 2000, **16**, 1354.
27 A. Campion and P. Kambhampati, *Chem. Soc. Rev.*, 1998, **27**, 241.
28 S. Nie and S. R. Emory, *Science*, 1997, **275**, 1102.
29 K. Kneipp, Y. Wang, H. Kneipp, I. Itzkan, R. R. Dasari and M. S. Feld, *Phys. Rev. Lett.*, 1996, **76**, 2444.
30 P. Dibrov, J. Dzioba, K. K. Gosink and C. C. Häse, *Antimicrob. Agents Chemother.*, 2002, **46**, 2668.
31 A. Panáček, L. Kvítek, R. Prucek, M. Kolář, R. Večeřová, N. Pizúrová, V. K. Sharma, T. Nevěčná and R. Zbořil, *J. Phys. Chem. B*, 2006, **110**, 16248.
32 N. Simonetti, G. Simonetti, F. Bougnoil and M. Scalzo, *Appl. Environ. Microbiol.*, 1992, **58**, 3834.
33 J. C. Grunlan, J. K. Choi and A. Lin, *Biomacromolecules*, 2005, **6**, 1149.
34 D. Gonnissen, A. Hubin and J. Vereecken, *Electrochim. Acta*, 1999, **44**, 4129.
35 R. D. Mondt, K. Baert, I. Geuens, L. van Vaeck and A. Hubin, *Langmuir*, 2006, **22**, 11360.
36 L. Delattre, C. Dubuy and F. Babonneau, *J. Sol–Gel Sci. Technol.*, 1994, **2**, 185–188.
37 Y. Saito, J. J. Wang, D. N. Batchelder and D. A. Smith, *Langmuir*, 2003, **19**, 6857–6861.
38 L. Kvitek, R. Prucek, A. Panáček, R. Novotný, J. Hrbác and R. Zbořil, *J. Mater. Chem.*, 2005, **15**, 1099.
39 C. M. Halliwell and A. E. G. Cass, *Anal. Chem.*, 2001, **73**, 2476.
40 S. L. Westcott, S. J. Oldenburg, T. R. Lee and N. J. Halas, *Langmuir*, 1998, **14**, 5396.
41 B. Kutsch, O. Lyon, M. Schmitt, M. Menning and O. Schmidt, *J. Non-Cryst. Solids*, 1997, **217**, 143.
42 M. Menning, M. Schmitt and O. Schmidt, *J. Sol–Gel Sci. Technol.*, 1997, **8**, 1035.
43 K. Yliniemi, P. Ebbinghaus, P. Keil, K. Kontturi and G. Grundmeier, *Surf. Coat. Technol.*, 2007, **201**, 7865.
44 SERS enhancement factor (EF) was calculated using the following equation:

$$EF = \frac{I(\text{surf})/(cN_a V(L))}{I(\text{bulk})/((A(L)R)/A_m)}$$

where $I(\text{surf})$ is the intensity of PMT on the surface, c is the concentration of PMT solution, N_a is Avogadro's number, $V(L)$ is the volume of the laser, $I(\text{bulk})$ is the intensity of pure PMT (powder), $A(L)$ is the area of the laser, R is the roughness and A_m is the size of the PMT molecule.
45 M. T. Madigan and J. M. Martinko, *Brock Biology of Microorganisms*, 11th edn, Pearson Education, Inc., New Jersey, 2006, pp. 677–679.